Fast Adaptation in Mouse Olfactory Sensory Neurons Does Not Require the Activity of Phosphodiesterase

Anna Boccaccio,[1] Laura Lagostena,[1] Volker Hagen,[2] and Anna Menini[1]

[1]International School for Advanced Studies, S.I.S.S.A., Sector of Neurobiology, 34014 Trieste, Italy
[2]Research Institute for Molecular Pharmacology, D-13125 Berlin, Germany

Vertebrate olfactory sensory neurons rapidly adapt to repetitive odorant stimuli. Previous studies have shown that the principal molecular mechanisms for odorant adaptation take place after the odorant-induced production of cAMP, and that one important mechanism is the negative feedback modulation by Ca^{2+}-calmodulin (Ca^{2+}-CaM) of the cyclic nucleotide-gated (CNG) channel. However, the physiological role of the Ca^{2+}-dependent activity of phosphodiesterase (PDE) in adaptation has not been investigated yet. We used the whole-cell voltage-clamp technique to record currents in mouse olfactory sensory neurons elicited by photorelease of 8-Br-cAMP, an analogue of cAMP commonly used as a hydrolysis-resistant compound and known to be a potent agonist of the olfactory CNG channel. We measured currents in response to repetitive photoreleases of cAMP or of 8-Br-cAMP and we observed similar adaptation in response to the second stimulus. Control experiments were conducted in the presence of the PDE inhibitor IBMX, confirming that an increase in PDE activity was not involved in the response decrease. Since the total current activated by 8-Br-cAMP, as well as that physiologically induced by odorants, is composed not only of current carried by Na^+ and Ca^{2+} through CNG channels, but also by a Ca^{2+}-activated Cl^- current, we performed control experiments in which the reversal potential of Cl^- was set, by ion substitution, at the same value of the holding potential, −50 mV. Adaptation was measured also in these conditions of diminished Ca^{2+}-activated Cl^- current. Furthermore, by producing repetitive increases of ciliary's Ca^{2+} with flash photolysis of caged Ca^{2+}, we showed that Ca^{2+}-activated Cl^- channels do not adapt and that there is no Cl^- depletion in the cilia. All together, these results indicate that the activity of ciliary PDE is not required for fast adaptation to repetitive stimuli in mouse olfactory sensory neurons.

The Journal of General Physiology

INTRODUCTION

Detection of odorants from the external environment begins in the olfactory sensory epithelium in the nasal cavity, where odorant molecules bind to odorant receptor proteins in the ciliary membrane of vertebrate olfactory sensory neurons, triggering the olfactory transduction cascade that produces an electrical signal. Adaptation to repetitive or maintained odorant stimuli starts at the level of olfactory sensory neurons through a Ca^{2+}-dependent modulation of the olfactory transduction cascade, although the two different types of adaptation could involve some different molecular mechanism.

Olfactory transduction involves the activation of odorant receptor–coupled GTP-binding protein, adenylate cyclase III, and the subsequent increase in the ciliary concentration of cAMP, which directly opens cyclic nucleotide-gated (CNG) channels, allowing a depolarizing influx of Na^+ and Ca^{2+} ions into the cilia. The increase in intraciliary Ca^{2+} concentration produces both excitatory and inhibitory effects (Schild and Restrepo, 1998; Menini, 1999; Firestein 2001; Matthews and Reisert, 2003; Menini et al., 2004). An excitatory action of the increase of Ca^{2+} concentration is the opening of Ca^{2+}-activated Cl^- channels and, since olfactory sensory neurons maintain an unusually high intraciliary concentration of Cl^- (Reuter et al., 1998; Kaneko et al., 2004), a consequent efflux of Cl^- from the cilia causes a further depolarizing current (Kleene and Gesteland, 1991; Kleene, 1993; Kurahashi and Yau, 1993; Lowe and Gold, 1993a; Frings et al. 2000). Recently, it has been shown that the Na-K-2Cl cotransporter NKCC1 is involved in the maintenance of a high Cl concentration inside olfactory sensory neurons (Reisert et al., 2005), although a very recent study indicates the possibility that NKCC1 is not the only component involved in this process (Nickell et al., 2006).

The Ca^{2+} inhibitory effects are mainly mediated by its binding to calmodulin (CaM). The feedback actions of the complex Ca^{2+}-calmodulin (Ca^{2+}-CaM) in the cilia include the inhibition of adenylate cyclase III by the Ca^{2+}-CaM-dependent protein kinase II (Wayman et al., 1995; Boekhoff et al., 1996; Wei et al., 1996, 1998), the enhancement of the activity of the ciliary phosphodiesterase

Correspondence to Anna Boccaccio: aboccac@sissa.it

Abbreviations used in this paper: BCMCM, [6,7-bis(carboxymethoxy) coumarin-4-yl]methyl; CaM, calmodulin; CNG, cyclic nucleotide-gated; PDE, phosphodiesterase.

PDE1C2 that hydrolyzes cAMP (Borisy et al., 1992; Yan et al., 1995), and a negative feedback modulation on the CNG channel (Kramer and Siegelbaum, 1992; Chen and Yau, 1994; Balasubramanian et al., 1996; Kleene, 1999; Bradley et al., 2001; Trudeau and Zagotta, 2003; Bradley et al., 2004).

The restoration of Ca^{2+} concentrations to basal levels occurs via a Na^+/Ca^{2+} exchanger, which extrudes Ca^{2+} from the olfactory cilia (Jung et al., 1994; Reisert and Matthews, 1998; Reisert and Matthews, 2001).

Olfactory sensory neurons have been shown to rapidly adapt to repetitive odorant stimuli (Kurahashi and Shibuya, 1990; Kurahashi and Menini, 1997; Leinders-Zufall et al., 1998; Ma et al., 1999; Reisert and Matthews, 1999; Reisert and Matthews, 2001; Ma et al., 2003). Kurahashi and Menini (1997) have investigated the molecular mechanisms of fast odorant adaptation and have shown that the reduction of the transduction current in the adapted state is attributable to processes occurring after the production of cAMP, and could be described by a negative feedback on cAMP-gated channels. They investigated the effects of Ca^{2+} occurring after the production of cAMP by activating the CNG channels directly by rapid and repetitive increments in cAMP concentrations through the photocleavage of caged cAMP in the olfactory cilia (Lowe and Gold, 1993a,b; Kurahashi and Menini, 1997; Takeuchi and Kurahashi, 2002, 2003, 2005; Lagostena and Menini, 2003).

In recent years, several studies have characterized in more detail the influence on adaptation of the negative feedback modulation by Ca^{2+}-CaM of the cAMP sensitivity of heteromeric olfactory CNG channels (Bradley et al., 2001, 2004, 2005; Munger et al., 2001). However, so far, the physiological role played in adaptation by the enhancement given by Ca^{2+}-CaM to the activity of the ciliary PDE1C2 (Borisy et al., 1992; Yan et al., 1995) has not been investigated. One way of testing the role of PDE1C2 in adaptation would be to compare the responses of PDE1C2-null mice with those of wild-type mice. In the absence of knock-out mice for PDE1C2, we chose instead a different strategy. We investigated the role of PDE1C2 in fast adaptation to repetitive stimuli by using 8-Br-cAMP to activate currents in the cilia because C-8–substituted derivatives of cyclic nucleotides are commonly used as hydrolysis-resistant compounds (Braumann et al., 1986; Butt et al., 1995; Beltman et al., 1995). Moreover, it is well established that 8-Br-cAMP is a potent agonist of the native olfactory CNG channel: it elicits the same maximal current as cAMP, the concentration activating half of the maximal current is ~5–10 times lower than that of cAMP, and the channel sensitivity to 8-Br-cAMP is modulated by Ca^{2+}-CaM similarly to cAMP (Balasubramanian et al., 1996). We produced rapid and repetitive amounts of 8-Br-cAMP in the cilia by photocleavage of [6,7-bis(carboxymethoxy)coumarin-4-yl]methyl (BCMCM)–caged 8-Br-cAMP. The total elicited current is composed, as the odorant-induced response, of two distinct inward currents: a first current flowing through CNG channels carried by Na^+ and Ca^{2+} into the cilia, followed by an efflux of Cl^- through channels activated by the increase in intracellular Ca^{2+}. With repetitive release of 8-Br-cAMP we reproduced previously measured properties of fast odorant adaptation, such as Ca^{2+} dependence, reduction in the amplitude of the adapted response, subsequent recovery to the control amplitude with prolonged intervals between stimuli, and shift of the dynamic range of the response. These results are consistent with the hypothesis that PDE1C2 does not play a relevant role in adaptation to repetitive stimuli. However, a study in retinal rods has shown that endogenous PDEs degrade 8-Br-cGMP, even though hydrolysis of 8-Br-cGMP proceeds at least 500 times more slowly than that of cGMP (Zimmerman et al., 1985). To our knowledge, there are no reports on the resistance to hydrolysis of 8-Br-cAMP by PDE1C2, and therefore we also performed control experiments using a broad range PDE inhibitor, IBMX, and found that adaptation to repetitive stimuli was still present.

Moreover, to clarify the contribution to adaptation of the cationic current through CNG channels and of the anionic current through Ca^{2+}-activated Cl^- channels, we performed additional experiments preventing the current contribution through Cl^- channels. We changed the Cl^- concentration to have a reversal potential for Cl^- equal to the holding potential of −50 mV; in these ionic conditions, the current was mainly carried by CNG channels and adaptation was still present, consistent with inhibition of CNG channels. Finally, we also directly investigated the possibility that Ca^{2+} could produce additional adaptation at the level of Ca^{2+}-activated Cl^- channels. We photoreleased Ca^{2+} from caged Ca^{2+} with repetitive flashes applied to the cilia and we measured the same peak amplitude responses, indicating that the Ca^{2+}-activated Cl^- channel did not contribute to adaptation.

Taken together, these results indicate that fast adaptation to repetitive stimuli in mouse olfactory sensory neurons does not require the activity of PDE. However, it should be noted that our results do not exclude the possibility that PDE plays a physiological role in adaptation in different experimental conditions, such as with long odorant exposures.

MATERIALS AND METHODS

Dissociation of Mouse Olfactory Sensory Neurons

Olfactory sensory neurons were dissociated enzymatically from the olfactory epithelium of 4–8-wk-old mice of the BALB/c strain, as previously described (Lagostena and Menini, 2003). In brief, mice were anesthetized with CO_2 inhalation, decapitated, and then the head was hemisected sagittally along the septum. The olfactory epithelium was removed and dissected at 4°C and minced with fine forceps in zero-divalent mammalian Ringer's solution

(in mM: 140 NaCl, 5 KCl, 10 HEPES, 1 EDTA, 10 glucose, 1 Na-pyruvate, pH 7.2). The tissue was incubated in 1 mM cysteine and 1 U/ml papain for 20 min at room temperature; the reaction was terminated with 1 ml of Ringer's solution (in mM: 140 NaCl, 5 KCl, 1 $CaCl_2$, 1 $MgCl_2$, 10 HEPES, 10 glucose, and 1 Na-pyruvate, pH 7.2) with 0.1 mg/ml BSA, 200 μg/ml leupeptin, and 0.025 mg/ml DNase I. Cells were carefully triturated with a flame-polished Pasteur pipette, filtered with cell strainer with 40 μm diameter pores to discard cells' agglomerates, centrifugated, and resuspended in Ringer's solution. Cells were then plated on glass coverslips coated with concanavalin A and poly-L-lysine to favor cell adhesion.

Before use, dissociated olfactory sensory neurons were allowed to settle for at least 45 min at 4°C. Dissociated preparations were constantly perfused with normal Ringer's solution (2 ml/min). Olfactory sensory neurons were observed with an inverted microscope (Olympus IX70) with an oil-immersion 100× objective (Olympus or Carl Zeiss MicroImaging, Inc.) and identified by their characteristic bipolar shape. Only olfactory sensory neurons with clearly visible cilia were used for the experiments. After the whole-cell configuration was reached, in some cases the neuron was detached from the bottom of the chamber. After the whole-cell configuration, olfactory sensory neurons sometimes rounded progressively and the dendrite partially retracted, as previously described (Dubin and Dionne 1994; Reisert and Matthews 1999).

Patch-clamp Recordings

Currents were measured with an Axopatch 200B or Axopatch 1D patch-clamp amplifier (Axon Instruments) in the whole-cell voltage-clamp mode. Patch pipettes were made using borosilicate capillaries (WPI) and pulled with a Narishige PP83 puller (Narishige), using a double stage pull. The diameter of the tip was ∼1 μm and the pipette resistances were 2–7 MΩ when filled with the standard intracellular solution. Currents were low-pass filtered at either 250 Hz or 1 kHz and acquired respectively at 500 Hz or 2 kHz by the analogue-to-digital interface Digidata 1322A (Axon Instruments). In a few cases, for current drawings, some data were digitally smoothed or a further filter was applied offline to remove 50 Hz due to perfusion. Acquisition and storage of data were performed with PClamp 8.2 software (Axon Instruments). All experiments were performed at room temperature (20–22°C).

Synthesis of Caged Cyclic Nucleotides

The caged cAMP and 8-Br-cAMP used in this study were the equatorial diastereomers of BCMCM-caged cAMP ([6,7-bis(carboxymethoxy)coumarin-4-yl]methyl adenosine 3′,5′-cyclic monophosphate) and of the BCMCM-caged derivative of the PDE-resistant 8-Br-cAMP, respectively. BCMCM-caged cAMP was prepared as previously described (Hagen et al., 2001). BCMCM-caged 8-Br-cAMP (axial diastereomer: ^{31}P NMR [DMSO-d_6] δ −4.68; ^{1}H NMR [DMSO-d_6] δ 4.33 [dt, J = 10.0 and 4 Hz, 1H], 4.43 [t, J = 10 Hz, 1H], 4.73–4.75 [m, 1H], 4.82 [s, 2H], 4.90 [s, 2H], 5.00 [d, J = 5 Hz, 1H], 5.48 [m, 2H], 5.59–5.62 [m, 1H], 5.92 [s, 1H], 6.46 [s, 1H], 7.09 [s, 1H], 7.23 [s, 1H], 7.68 [br s, 2H], 8.14 [s, 1H]; UV [HEPES buffer, pH 7.2] λ_{max} [ε] 347 nm [10300 $M^{-1}cm^{-1}$]; equatorial diastereomer: ^{31}P NMR [DMSO-d_6] δ −2.65; ^{1}H NMR [DMSO-d_6] δ 4.41 [q, J = 10.0 Hz, 1H], 4.52–4.56 [m, 1H], 4.77–4.80 [m, 1H], 4.81 [s, 2H], 4.90 [s, 2H], 5.05 [d, J = 5 Hz, 1H], 5.42 [d, J = 7 Hz, 2H], 5.49–5.52 [m, 1H], 5.92 [s, 1H], 6.39 [s, 1H], 7.08 [s, 1H], 7.21 [s, 1H], 7.65 [br s, 2H], 8.23 [s, 1H]; UV [HEPES buffer, pH 7.2] λ_{max} [ε] 346 nm [10000 $M^{-1}cm^{-1}$]) was synthesized in analogy to BCMCM-caged cAMP by reaction of the free acid of 8-Br-cAMP and [6,7-bis(*tert*-butoxycarbonylmethoxy)coumarin-4-yl]diazomethane, diastereomer separation using preparative reverse-phase HPLC and subsequent deprotection of the tert-butoxy groups with trifluoroacetic acid. The yield was 15.8%. The two caged compounds exhibited remarkable photochemical properties, like rapid release of the cyclic nucleotides (the photoconversion takes place within a few nanoseconds), high efficiency of photocleavage, long-wavelength absorption maxima and high solubility as well as stability in aqueous solutions (Hagen et al., 2005).

Photolysis of Caged Compounds

For flash photolysis of the caged compounds we used a xenon flash-lamp system JML-C2 (Rapp OptoElectronic GmbH) coupled with the epifluorescence port of the microscope with a quartz light guide. The spot of light had a diameter of ∼15 μm that could cover only the ciliary region or also part of the dendrite. Given the very small size of mouse olfactory sensory neurons it was sometimes technically difficult to restrict the illumination area to the cilia only. Moreover after obtaining the whole-cell configuration, sometimes the dendrite retracted and also part of the body was illuminated by the flash.

The released energy at the objective was of few mJ, and this was reduced to an unknown grade of intensity inside the cilia. The flash duration was <1.5 ms and was kept constant during each experiment. The light intensity was controlled by neutral-density filters (Omega Optical or Glen Spectra) capable of reducing the maximal intensity in the range from 0.1 to 89% of its value and by changing the settings of the flash lamp, spanning a range of ∼40 times. The filter integrity was tested by using a photodiode. The interval between experiments was at least 2 min in order to allow the cell to recover completely from adaptation.

Solutions

The extracellular mammalian Ringer solution contained (in mM): 140 NaCl, 5 KCl, 1 $CaCl_2$, 1 $MgCl_2$, 10 HEPES, 10 glucose, and 1 sodium pyruvate, pH 7.4. The composition of the nominally 0 Ca^{2+} extracellular solution was similar except that it contained 10 mM EGTA and no added Ca^{2+}. Whole-cell pipette solution contained (in mM): 145 KCl, 4 $MgCl_2$, 0.5 EGTA, 10 HEPES, 1 MgATP, 0.1 GTP, pH 7.4. In some experiments, intracellular free Ca^{2+} concentration was buffered to ∼100 nM by adding 0.24 mM $CaCl_2$ (MaxChelator, http://www.stanford.edu/~cpatton/maxc.html). In the experiments designed to separate cationic from anionic currents, we replaced part of the intracellular chloride with gluconate (Vrev for chloride = −50 mV). The pipette gluconate-solution contained (in mM): 12 KCl, 133 potassium gluconate, 4 $MgCl_2$, 0.24 $CaCl_2$, 0.5 EGTA, 10 HEPES, 1 MgATP, 0.1 GTP, pH 7.4 (calculated free Ca^{2+} 84 nM with MaxChelator). Osmolarity was adjusted to 310 mOsm for the extracellular and to 290 mOsm for the intracellular solution. Liquid junction potential was corrected off-line for the experiments performed with the gluconate intracellular solution.

The caged cyclic nucleotides BCMCM-cAMP and BCMCM-8-Br-cAMP were dissolved in DMSO at 50 or 10 mM and stored at −20°C for up to 3 mo. The final concentrations, 50 μM for BCMCM-8-Br-cAMP and varying from 50 μM to 250 μM for BCMCM-cAMP, were obtained by diluting an aliquot of the stock solution into the pipette solution, kept refrigerated in the dark during the experimental session, and stored for a few days at −20°C.

The intracellular recording solution for the photorelease of caged Ca^{2+} contained (in mM): 3 DMNP-EDTA, 1.5 $CaCl_2$, 140 KCl, 10 HEPES, pH 7.4. DMNP-EDTA was purchased from Molecular Probes-Invitrogen, and $CaCl_2$ was adjusted with a 0.1 M standard solution from Fluka.

The caged compounds were allowed to diffuse freely from the patch pipette into the cytoplasm of an olfactory sensory neuron for at least 2 min after establishment of the whole-cell configuration.

The adenylate cyclase inhibitors MDL-12,330A and SQ 22,536 were dissolved in Ringer solution and used at a final concentration of 50 and 100 μM, respectively. IBMX was dissolved in DMSO

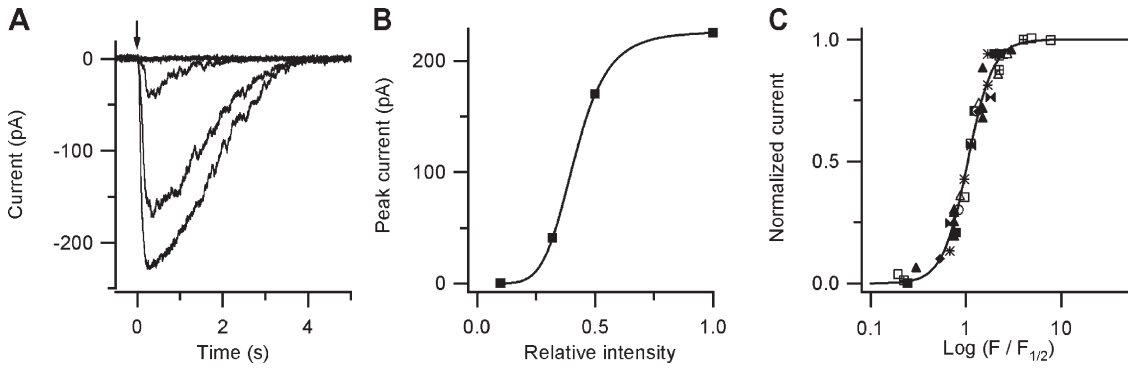

Figure 1. Current responses induced by photorelease of 8-Br-cAMP as a function of flash intensity. (A) 50 μM caged 8-Br-cAMP diffused into the cell from the patch pipette and flashes of increasing intensity and identical duration were applied to the ciliary region. The arrow indicates the time of application of light flashes of various relative intensities: 0.1, 0.32, 0.5, and 1. Whole-cell current responses were measured at the holding potential of −50 mV. (B) Peak currents from the cell in A were plotted as a function of the relative light intensity, F. The continuous line was the best fit of the Hill Eq. 1 to the data with the following values: I_{max} = 226 pA, $F_{1/2}$ = 0.41, and n = 5.4. (C) Collected results from nine different olfactory sensory neurons. Each symbol represents a different cell. Both axes are normalized values. Normalized peak currents in each cell (I/I_{max}) were plotted versus the logarithm of the relative intensity normalized to the $F_{1/2}$ value ($F/F_{1/2}$) for each cell. The continuous line was the best fit of Eq. 1 to the collected data with n = 3.3. Values of $F_{1/2}$ ranged from 0.10 to 0.47, n from 3 to 5.4, and I_{max} from −160 to −1200 pA.

at 100 mM and an aliquot was added to Ringer solution to a final concentration of 300 μM.

Chemicals, except for caged cyclic nucleotides or otherwise stated, were purchased from Sigma-Aldrich.

Data Analysis

Data analysis and figures were made with Igor software (Wavemetrics). Current amplitudes at each holding potential were calculated by subtracting the value of the baseline. Averages were shown ± standard deviation and the total number of neurons (N).

RESULTS

Responses of Olfactory Sensory Neurons to Photorelease of 8-Br-cAMP in the Cilia

Fig. 1 A shows the current responses of one olfactory sensory neuron to photorelease of 8-Br-cAMP in the cilia. Various concentrations of 8-Br-cAMP were obtained by using neutral density filters to reduce the maximal intensity of light. Peak amplitudes were found to increase with flash intensity. Peak current amplitudes were plotted as a function of the relative light intensity, F, in Fig. 1 B for the cell shown in A (see also Fig. 7). Data were fitted by the Hill equation:

$$I/I_{max} = F^n/(F^n + F_{1/2}^n), \quad (1)$$

where I is the peak current measured at the relative light intensity F, I_{max} is the maximal measured peak current, $F_{1/2}$ is the relative intensity producing 50% of I_{max}, and n is the Hill coefficient. The best fit gave I_{max} = 226 pA, $F_{1/2}$ = 0.41, and n = 5.4 Similar relations between light intensity and current response were measured in a total of nine different olfactory sensory neurons. The average value for the Hill coefficient was n = 4.0 ± 0.8 (N = 9). In Fig. 1 C, data from the nine neurons were combined and plotted as normalized peak currents (I/I_{max}) versus normalized relative flash intensities ($F/F_{1/2}$).

The total current induced by photorelease of 8-Br-cAMP is due, similarly to the odorant-induce current, to the sequential activation of two types of channels in a nonlinear fashion. CNG channels are activated first, followed by the activation of Ca^{2+}-activated Cl channels.

To obtain an estimate of the cytoplasmic concentration of 8-Br-cAMP photoreleased inside the cilia, we modified the experimental conditions to measure only the contribution of CNG channels to the elicited current. Then, assuming that the relation between photoreleased cyclic nucleotide and flash intensity is linear (Lowe and Gold, 1993a), we estimated the 8-Br-cAMP concentration by comparing the normalized current at various flash intensities with the known dose–response relation for the native olfactory CNG channel. To avoid activation of Ca^{2+}-activated Cl^- channels, we prevented Ca^{2+} entry through the CNG channels recording in nominally 0 Ca^{2+} extracellular solutions in the presence of 10 mM EGTA and in the absence of added Ca^{2+}. Currents induced by various light intensities at a holding potential of −50 mV (Fig. 2, A–C) were measured and fitted by the Hill equation (Eq. 1). The average Hill coefficient was reduced from the average value of 4.0 ± 0.8 in Ringer solution to 1.9 ± 0.4 in 0 Ca^{2+}, consistent with the reduction in the nonlinear amplification due to the absence of activation of the Cl^- component. To obtain an estimate of the cytoplasmic concentration of photoreleased 8-Br-cAMP, we compared our data with dose–response relationships for 8-Br-cAMP measured, in the absence of Ca^{2+},

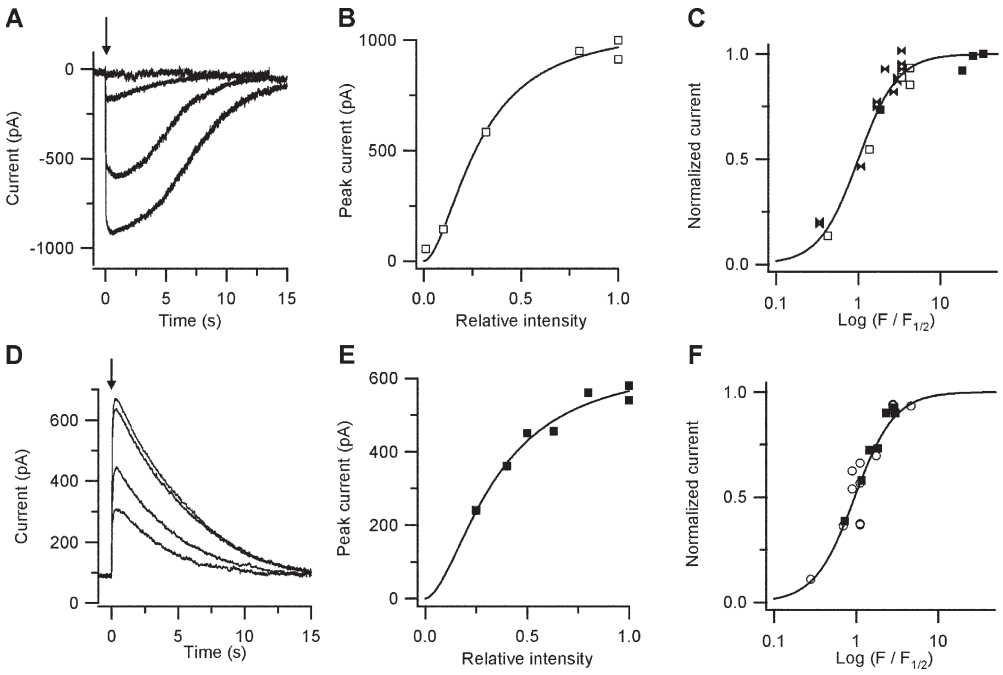

Figure 2. Estimation of the photoreleased concentration of 8-Br-cAMP. (A–C) Current responses in 0 Ca^{2+} Ringer solution (with 10 mM EGTA) induced by photorelease of 8-Br-cAMP as a function of flash intensity at −50 mV. In the absence of Ca^{2+} entry, the current was entirely due to CNG channels. (D–F) Ca^{2+} entry was also reduced by recording at +50 mV in Ringer solution. (A and D) Arrows indicate the time of application of light flashes of various relative intensities: 0.01, 0.1, 0.32, and 0.8 in A and 0.25, 0.4, 0.8, and 1 in D in two different neurons. Peak currents from the experiments in A and D were plotted as a function of the relative light intensity in B and E, respectively. The continuous line was the best fit of the Hill Eq. 1 to the data with the following values: (B) I_{max} = 1070 pA, $F_{1/2}$ = 0.28, n = 1.8; (E) I_{max} = 653 pA, $F_{1/2}$ = 0.34, n = 1.7. Collected results from data at −50 mV in 0 Ca^{2+} solution from three different olfactory sensory neurons (C), and from data at +50 mV in Ringer solution from two different olfactory sensory neurons (D). Each symbol represents a different cell. Both axes are normalized values. Normalized peak currents in each cell (I/I_{max}) were plotted versus the logarithm of the relative intensity normalized to the $F_{1/2}$ value ($F/F_{1/2}$) for each cell. The continuous line was the best fit of Eq. 1 to the collected data with n = 1.8 in C and 1.7 in F. The average value for n was 1.9 ± 0.4 (N = 3) at −50 mV and 0 Ca^{2+} solution, and 1.7 ± 0.1 (N = 2) at +50 mV in Ringer solution.

in excised inside-out patches at −50 mV in the rat: $K_{1/2}$ = 0.37 μM, n = 1.9 (Balasubramanian et al., 1996), or in the mouse: $K_{1/2}$ = 0.8 μM, n = 1.4 (Pifferi et al. 2006). We estimated that the maximal photoreleased concentration of 8-Br-cAMP varied between ∼5 and 10 μM.

Since olfactory sensory neurons often became very unstable in the absence of Ca^{2+} and in the presence of 10 mM EGTA in the extracellular solution, we also used a different experimental protocol to diminish Ca^{2+} entry and subsequent Cl^- current activation. Experiments were performed in Ringer solution at the holding potential of +50 (Figs. 2, D–F). In these conditions, the influx of Ca^{2+} through CNG channels is greatly reduced and the outward current is mainly carried by K ions, whose permeation through CNG channels is similar to that of Na ions (Kaupp and Seifert, 2002). In these experimental conditions, the average Hill coefficient was reduced from 4.0 ± 0.8 in Ringer at −50 mV to 1.7 ± 0.1 in Ringer at +50 mV, consistent with the reduced Ca^{2+} entry and the absence of activation of the Cl^- component, as in Fig. 2 C. The comparison with dose–response relationships for 8-Br-cAMP measured at +50 mV in excised inside-out patches in the mouse $K_{1/2}$ = 0.4 μM, n = 1.2 for 8-Br-cAMP at +50 mV (Pifferi et al. 2006), produced an estimated maximal photoreleased concentration of 5–7 μM.

To obtain an estimation of the released concentration at a given intensity, it should be noted that since in different cells $F_{1/2}$ varied, the dose–response in the absence of Ca^{2+} per each individual cell should be measured.

Kinetics of Recovery to Baseline in Nominally 0 Ca^{2+}

We found a large variability in the time necessary for the current to return to baseline both in nominally 0 Ca^{2+} and Ringer solutions. In the absence of added Ca^{2+} and in the presence of 10 mM EGTA Ca^{2+} does not enter into the cilia, and therefore both its excitatory and its inhibitory actions are precluded. In these ionic conditions, the recovery of the current to baseline is likely to be mainly due to the decrease in the intraciliary concentration of 8-Br-cAMP due to diffusion from the cilia to the cell body (Chen et al., 1999). Fig. 3 shows recordings from one cell in which the current, in 0 Ca^{2+}, has already reached the maximal value at 50% of the maximal light intensity. Higher light intensities such as 80%, and 100% produced the same current peak, but caused an increase in the time necessary for the current to return to baseline. The observation that the time required for recovery to baseline after the flash is longer for higher light intensities indicates that although the CNG current was already fully activated, the intraciliary concentration of 8-Br-cAMP could be further increased.

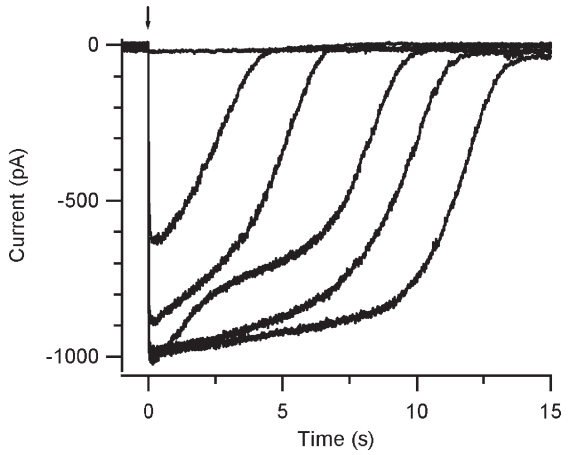

Figure 3. Kinetics of current recovery to baseline in 0 Ca^{2+} Ringer. Current responses induced by photorelease of 8-Br-cAMP as a function of flash intensity in 0 Ca^{2+} Ringer. Holding potential was −50 mV. Flashes of increasing relative intensities 0.01, 0.1, 0.32, 0.5, 0.8, 1 were applied to the ciliary region. In this neuron, the maximal current response, entirely due to activation of CNG channels, was already reached at 0.5 relative light intensity. Higher light intensities elicited the same peak current, but increased the time necessary for the current to return to baseline, probably due to the time employed by 8-Br-cAMP to diffuse away from the cilia. The increase in recovery time with higher light intensity indicates that although the CNG current was already fully activated, the intraciliary concentration of 8-Br-cAMP could be further increased, meaning that with a pipette concentration of 50 μM caged 8-Br-cAMP, the range of light intensity of our experimental system could fully activate the CNG channels.

Adaptation: Responses to Repetitive Stimuli

Fig. 4 shows adaptation measured in Ringer solution in response to two repetitive identical flashes photoreleasing 8-Br-cAMP (Fig. 4, A and C) or cAMP (Fig. 4, B and D) and the absence of adaptation in nominally 0 Ca^{2+} solution (Fig. 4 E). Since 8-Br-cAMP is ∼5–10 times more efficient than cAMP in activating olfactory CNG channels (Balasubramanian et al., 1996; Pifferi et al., 2006), in these experiments a higher concentration of caged cAMP (250 μM) than caged 8-Br-cAMP (50 μM) was included in the patch pipette to obtain free ciliary cyclic nucleotide concentrations activating CNG channels with a similar open probability. In Fig. 4 (A and B), recordings in 8-Br-cAMP were obtained with an interflash interval of ∼20 s, both at the holding potential of −50 mV and, to reduce the Ca^{2+} influx, of +50 mV. In Fig. 4 A at +50 mV (top trace), the peak responses to the first and second flash had similar values of 159 and 149 pA, respectively. On the contrary, at the holding potential of −50 mV (bottom trace), the peak response to the first flash was −951 pA, while the second flash produced a smaller current of −402 pA, therefore reducing the current to 42% of its initial value. Fig. 4 B shows currents induced by cAMP in a different neuron at the same 20-s interflash interval. In the illustrated neuron, results were similar to those shown in Fig. 4 A for 8-Br-cAMP: at +50 mV, repetitive flashes produced similar peak currents (116 and 107 pA), whereas at −50 mV, the second flash induced a peak current (−160 pA) that was 38% of that caused by the first flash (−421 pA). At −50 mV, similar results were obtained in five neurons for 8-Br-cAMP and in three neurons for cAMP. Fig. 4 (C and D) illustrates neurons in which interflash intervals of 5–6 s induced similar adaptation in 8-Br-cAMP and cAMP. Similar results were measured in 10 neurons for 8-Br-cAMP and in 5 neurons for cAMP. As previously noted for the dose–response relations, the heterogeneity of responses is likely to be due to several reasons: illumination of the neurons, percentage of CNG, and Ca^{2+}-activated Cl^- current. To measure adaptation to repetitive photoreleases of cyclic nucleotides, it is critical to determine if it is possible to obtain reproducible concentrations of cyclic nucleotide with each flash. Control experiments were performed in nominally 0 Ca^{2+} solution, where the absence of Ca^{2+} entry prevents both adaptation and activation of Ca^{2+}-activated Cl^- channels, and therefore currents are entirely due to activation of CNG channels only. Repetitive flashes of the same light intensity produced similar peak currents both at +50 mV (226 and 225 pA) and at −50 mV (−306 and −290 pA), indicating that the same cyclic nucleotide concentration was released (Fig. 4 E).

These results are in general agreement with previous observations that odorant adaptation is Ca^{2+} dependent and that, at sufficiently high positive potentials, it is not present (Kurahashi and Menini, 1997; Takeuchi and Kurahashi, 2003). Indeed at +50 mV, Ca^{2+} influx is much smaller than at −50 mV, and intracellular Ca^{2+} concentration does not reach a level sufficient to induce adaptation.

Fig. 5 shows responses in Ringer solution to two identical flashes at various relative light intensities in the same neuron. The percentage of current reduction after the second pulse was not the same at different light intensities: 31% at 0.25, 22% at 0.5, and 43% at 1 relative light intensities. Peak currents depend both on the released concentration of 8-Br-cAMP and on the amount of Ca^{2+} entering the cell, producing both inhibitory and excitatory effects. Indeed, the current reduction measured in Ringer solution to the second of a paired pulse is likely to be due both to a reduction in CNG current, and also to a reduction in Ca^{2+}-activated Cl^- currents related to a decreased Ca^{2+} influx through the CNG channels. We will present data showing that adaptation is primarily due to the inhibitory Ca^{2+} effect on the CNG channel (Fig. 9).

The amplitude of the adapted current response progressively recovered to the control value as the time interval between repetitive stimuli was increased. As previously shown (Fig. 4), responses are heterogeneous and, as a consequence, the time necessary to recover from adaptation is not the same in every cell, as it

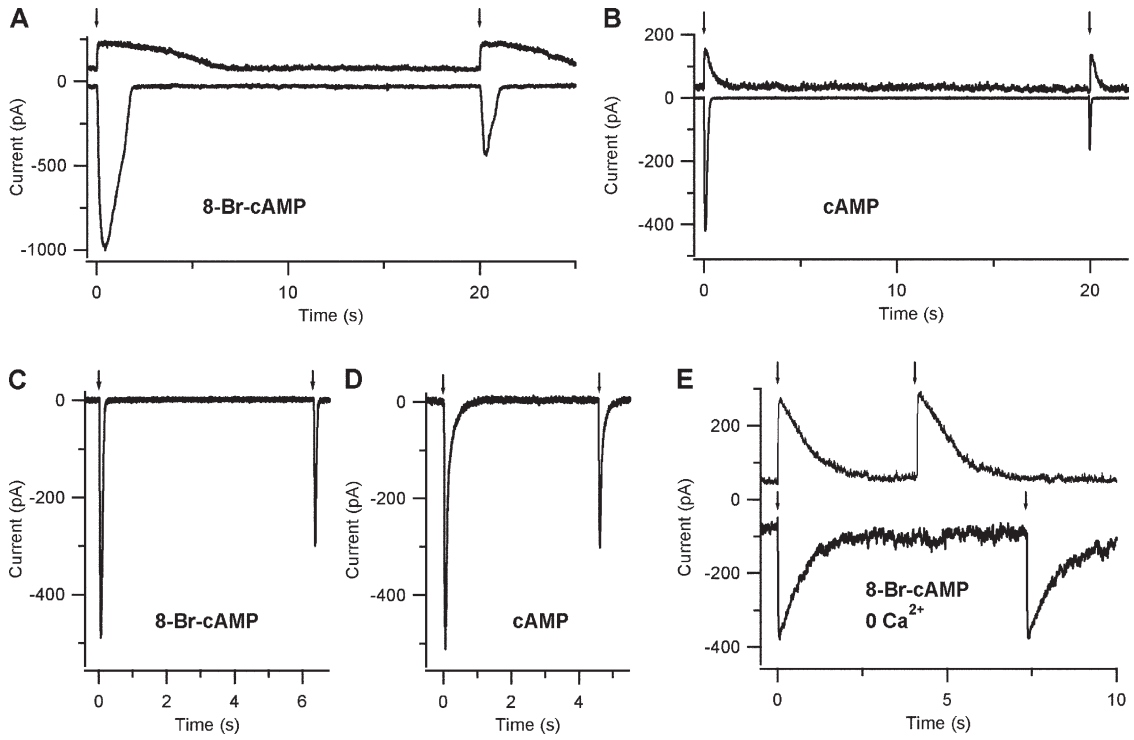

Figure 4. Response adaptation to photorelease of cAMP or 8-Br-cAMP. Different olfactory sensory neurons were loaded with 50 μM caged 8-Br-cAMP (A, C, and E) or with 250 μM caged cAMP (B and D). A and B show current responses to repetitive light flashes of the same maximal intensity at interflash interval of 20 s in two neurons with similar adaptation properties. In each panel, recordings at +50 mV (top traces) and at −50 mV (bottom traces) were obtained from the same neuron. The two selected neurons showed similar adaptation in 8-Br-cAMP (A) and cAMP (B). At −50 mV, the peak amplitudes of the responses to the second flash (−403 pA, −160 pA) were 42% and 38% of the responses to the first flash (−951 pA, −421 pA) for 8-Br-cAMP (A) or cAMP (B), respectively. At +50 mV, the peak amplitudes of current responses to repetitive flashes were very similar, indicating the absence of adaptation. C and D show two neurons in which adaptation was measured at interflash intervals of 6.3 s (C) or 4.6 s (D). The two selected neurons showed similar adaptation in 8-Br-cAMP (C) and cAMP (D). At −50 mV, the peak amplitudes of the responses to the second flash (−298 pA, −302 pA) were 61% and 59% of the responses to the first flash (−488 pA, −511 pA) for 8-Br-cAMP (C) or cAMP (D), respectively. (E) Control experiment in a different neuron in nominally 0 Ca^{2+} Ringer solution, where the absence of Ca^{2+} entry prevented both adaptation and the activation of the Ca^{2+}-activated Cl^- channel. Currents to repetitive flashes of the same maximal intensity photoreleasing 8-Br-cAMP reached a similar amplitude both at +50 mV (226 and 225 pA), and at −50 mV (−306 and −290 pA), indicating the photorelease of the same 8-Br-cAMP concentration. Control experiments in 0 Ca were obtained in a total of five neurons.

depends on the released concentration of cyclic nucleotides, on the amount of Ca^{2+} entering the cell, and its relative inhibitory and excitatory effects. Fig. 6 illustrates the responses to two identical flashes photoreleasing 8-Br-cAMP at various time intervals in one olfactory sensory neuron. When the interval between flashes was 2.5 s, the peak amplitude response to the second flash was reduced to 38% of the response to the first flash. The adapted response progressively recovered to 50% of the control with a time interval between flashes of 4 s, and to 71% when the time interval was 6.8 s. In Fig. 6 B, the responses shown in A were plotted superimposed. Similar results were measured in seven neurons for 8-Br-cAMP and in four neurons for cAMP. These results are in general agreement with previously published results measuring the time necessary for recovery from fast odorant adaptation of olfactory sensory neurons both in amphibians (Kurahashi and Menini, 1997; Leinders-Zufall et al., 1998; Takeuchi and Kurahashi, 2003) and in mammals (Ma et al., 1999). However, we have also found that in some neurons (Fig. 4), the time necessary for the current to recover from adaptation was longer, and it is likely that a similar range will be found with investigations of odor responses on a longer time scale.

Adaptation: Shift of the Dynamic Range

Sensory adaptation is not merely a reduction in response amplitude, but it involves the adjustment of the response to allow a cell to work over a broad range of stimuli (for review see Torre et al., 1995). Indeed, in odorant adaptation to repetitive stimuli there is a shift of the dynamic range (i.e., the range of stimulus concentrations over which the olfactory sensory neuron is able to respond) toward higher odorant concentrations compared with the control state (Kurahashi and Menini, 1997; Reisert and Matthews, 1999).

To examine whether the current reduction measured in repetitive photoreleases of 8-Br-cAMP (Figs. 4–6) was

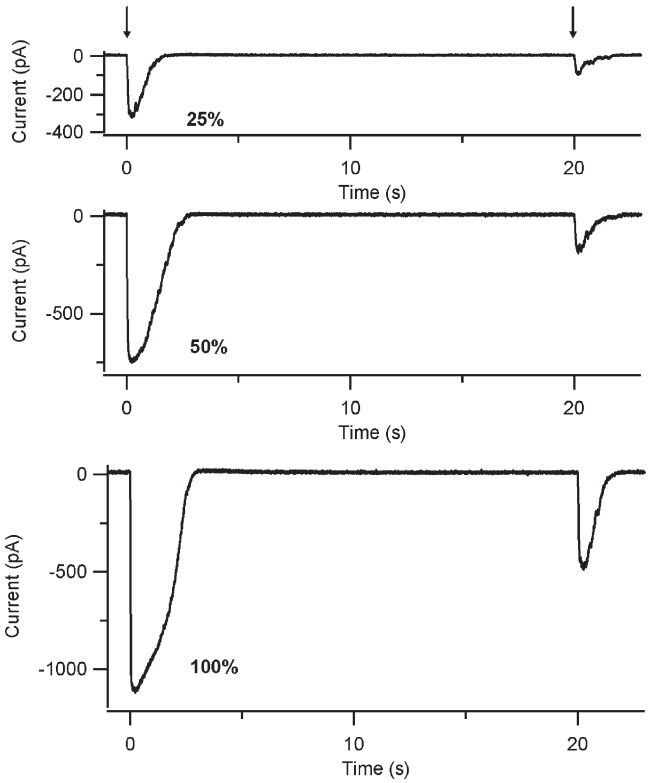

Figure 5. Response adaptation at different light intensities. Whole-cell currents induced by repetitive photorelease of 8-Br-cAMP in an olfactory sensory neuron held at −50 mV. The arrows indicate the timing of the light flashes at 0.25 (top trace), 0.5 (middle trace), and 1 (bottom trace) relative light intensities. Response adaptation was measured at interflash interval of 20 s. The peak amplitude of the adapted response was 31%, 22%, and 43% of the control response at 0.25, 0.5, and 1 relative light intensities, respectively.

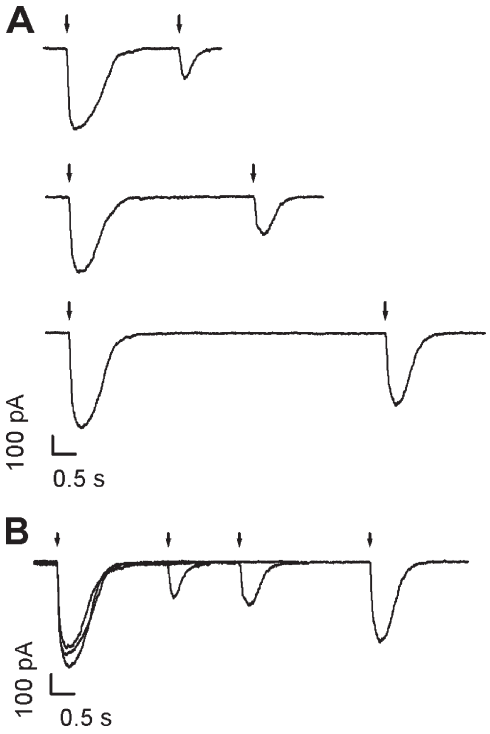

Figure 6. Time course of recovery from adaptation. (A) Responses to photorelease of 8-Br-cAMP were obtained with two light flashes of the same intensity at various time intervals 2.5, 4, and 6.8 s in the same olfactory sensory neurons. Traces in A are shown superimposed in B. Arrows indicate the timing of the light flashes. The holding potential was −50 mV.

due to a simple reduction of peak current amplitude or was instead caused by a shift of the dynamic range of the response, we measured the relation between flash intensity and response in the same olfactory sensory neuron first in the control state (as in Fig. 1) and then in the adapted state. Fig. 7 shows current responses and dose–response relations from two different olfactory sensory neurons in the control and in the adapted state. A dose–response in the control state was measured by photoreleasing 8-Br-cAMP at various light intensities (Fig. 7, A and E). Each olfactory sensory neuron was then adapted by photoreleasing 8-Br-cAMP with a first light flash of the maximal intensity, and then a second flash of various light intensities was applied, as illustrated in Fig. 7 (C and G). The current responses measured in the adapted state at the same relative light intensities as in the control state were plotted superimposed in Fig. 7 (B and F). A comparison between Fig. 7 (A and B) for one neuron and Fig. 7 (E and F) for a different neuron shows that the same relative flash intensity produced very different responses in the presence of the adapting stimulus. For example, for the first neuron, a relative intensity of 0.5 in the control state produced 80% of the maximal current, whereas in the adapted state, the current was only 5% of the maximal current in the control state (Fig. 7 C). In the second neuron, a relative intensity of 0.5 had already produced the maximal current, whereas in the adapted state, the current was reduced to ∼30% of the maximal value (Fig. 7 G). A plot of the current as a function of flash intensity in the control and in the adapted state (Figs. 7 D, H) revealed the expected shift of the dynamic range. Therefore, in the adapted state, the response range varied and higher flash intensities, releasing higher 8-Br-cAMP concentrations, were necessary to induce a response of the same amplitude as in the control state.

Data obtained from different neurons are usually not quantitatively comparable because the amount of shift of the dose response varied from cell to cell.

Inhibition of PDE by IBMX

The experiments illustrated in Figs. 4–7 show that also in the presence of 8-Br-cAMP, adaptation was measured. If 8-Br-cAMP is poorly hydrolyzable by PDE1C2, our results are consistent with the hypothesis that PDE1C2 activity is not necessary for fast response adaptation. However, since there is no direct demonstration that

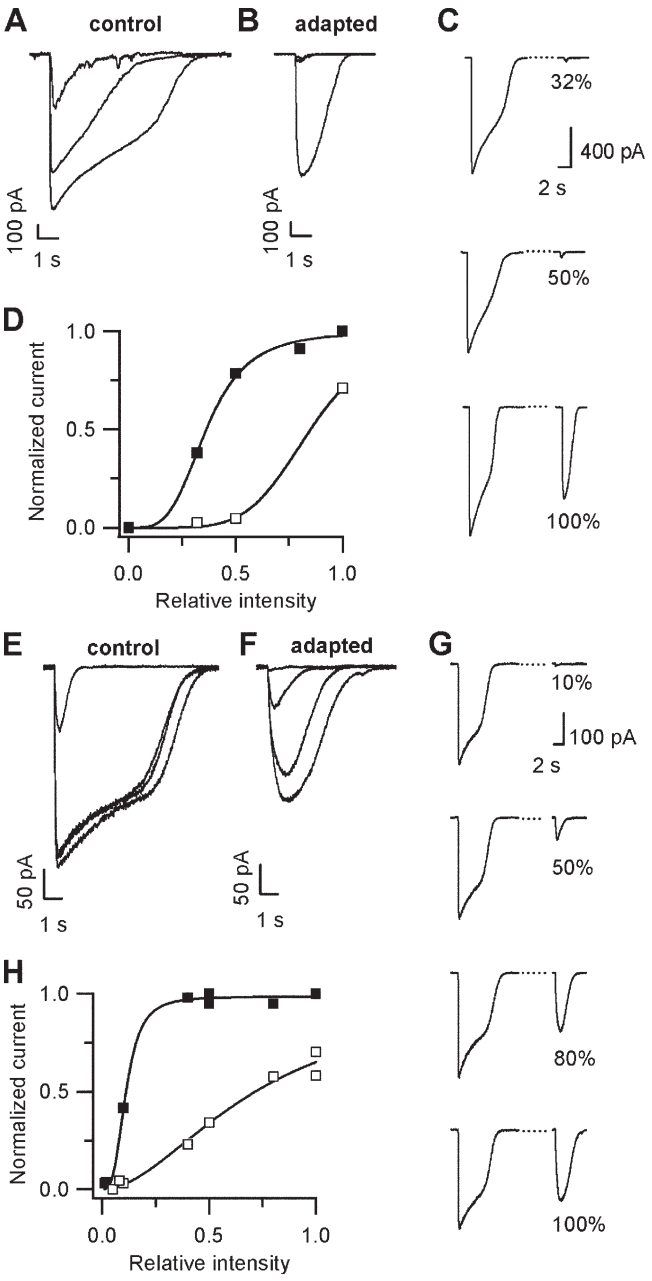

Figure 7. Shift of the dynamic range. Current responses induced by photolysis of caged 8-Br-cAMP in two olfactory sensory neurons. Currents were measured as a function of relative flash intensities in control and in adapted condition for the first (A–D) and the second (E–H) olfactory neuron, respectively. Relative flash intensities were 0.32, 0.50, and 1 in the first neuron (A and B), with $I_{max} = -1150$ pA, and 0.1, 0.5, 0.8, and 1 in the second neuron (E and F), with $I_{max} = -340$ pA. The superimposed current responses in the adapted state were obtained from the experiments illustrated in C and G: an adapting flash of maximal light intensity was applied to the neuron followed by a second flash after 19 s in C and 30 s in G. The intensity of the first flash was kept constant and the intensity of the second flash was varied as indicated in the figure. The holding potential was −50 mV. (D and H) Normalized peak currents were plotted versus relative flash intensity both for the control (filled squares) and for the adapted (open squares) state. Data were fitted by the Hill equation, Eq. 1, with $F_{1/2} = 0.36$ and $n = 3.7$ in the control, and with $F_{1/2} = 0.85$ and $n = 5.5$ in the adapted state for the first neuron (D), and with $F_{1/2} = 0.11$ and $n = 3.2$ in the control, and with $F_{1/2} = 0.72$ and $n = 1.9$ in the adapted state for the second neuron (H). Results showing a shift of the dynamic range in the adapted state toward higher light intensities compared with the control state were measured in three olfactory sensory neurons.

8-Br-cAMP is resistant to hydrolysis by PDE1C2, we also investigated the role of PDE in fast adaptation by using the PDE inhibitor IBMX to further reduce the possibility that PDE1C2 in the cilia could hydrolyze 8-Br-cAMP. It is well known that application of IBMX often evokes a current in olfactory sensory neurons (Firestein et al. 1991a,b; Lowe and Gold 1993a). Indeed, in the cilia of olfactory sensory neurons there is an endogenous activity of both adenylate cyclase and PDE, and, in the presence of IBMX, the intraciliary cAMP concentration increases due the basal production of cAMP. To prevent the endogenous production of cAMP, we pretreated olfactory sensory neurons with the adenylate cyclase antagonists SQ 22,536 (Harris et al., 1979) or MDL-12,330A (Guellaen et al., 1977). The actions of the two antagonists have been investigated systematically in olfactory sensory neurons and it has been shown that both antagonists specifically block cAMP formation without affecting the olfactory CNG channel (Chen et al., 2000). After pretreatment with SQ 22,536 or MDL-12,330A to inhibit adenylate cyclase, we added IBMX to the bath solution to inhibit PDE. Fig. 8 shows the responses evoked by repetitive photorelease of 8-Br-cAMP at a holding potential of −50 mV. The response to the first flash was −900 pA and to the second flash was −265 pA, corresponding to a current reduction to 29% of its initial value. The occurrence of adaptation to repetitive pulses in the presence of IBMX provides a further indication that PDE activity is not necessary for olfactory adaptation.

Changing the Reversal Potential for Cl^-

The current elicited by 8-Br-cAMP is composed both of a cationic component through CNG channels and of an anionic component through Ca^{2+}-activated Cl^- channels. The measured adaptation in the presence of 8-Br-cAMP, even upon addition of IBMX to further inhibit PDE1C2 hydrolysis, could also be due to a Ca^{2+}-mediated effect on the Cl^- current instead than on the CNG channel. To investigate this possibility, we decreased Cl^- permeation by shifting the reversal potential of the Cl^- current to −50 mV, by using an intracellular solution where most of the Cl^- was replaced with gluconate. Fig. 9 shows the responses to two identical flashes applied to photorelease 8-Br-cAMP at +50 or −50 mV. At the holding potential of +50 mV (top trace), the peak responses to repetitive flashes had a similar amplitude of ∼80 pA. At the holding potential of −50 mV (bottom trace), corresponding to the calculated reversal potential for Cl^-, the peak response to the first flash was −22 pA and that to the

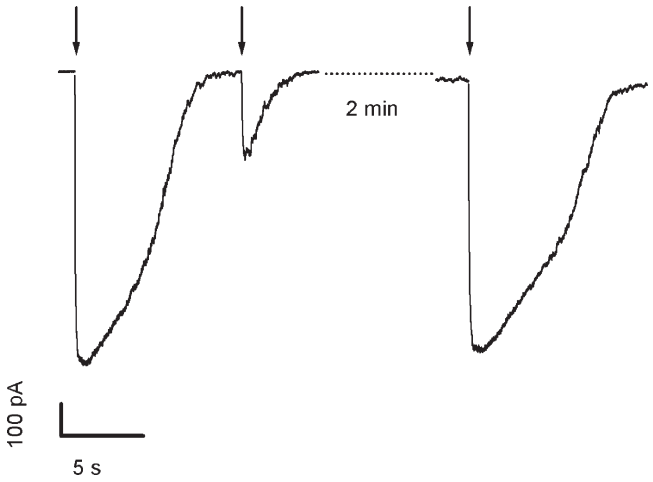

Figure 8. Response adaptation in the presence of the PDE inhibitor IBMX. Adaptation of the responses to photorelease of 8-Br-cAMP at −50 mV in presence of IBMX (300 μM) and MDL-12,330A (50 μM) in the bath. Interflash interval 10 s. The peak amplitude of the response to the second flash (−265 pA) was reduced to 29% of the response to the first flash (−914 pA). After 2 min, the response recovered to its initial value. Five olfactory sensory neurons were tested with repetitive flashes in the presence of IBMX and MDL-12,330A (two neurons) or SQ 22,536 (three neurons) and all showed adaptation.

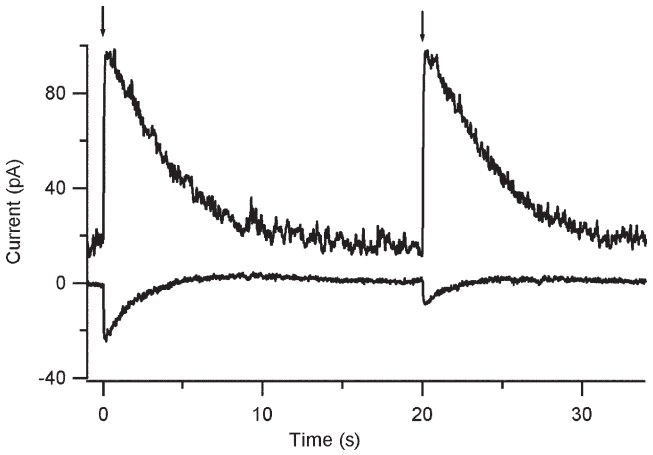

Figure 9. Response adaptation of the cationic current component. The reversal potential of the Cl^- current was set at −50 mV, reducing the intracellular Cl^- concentration by partial replacement with gluconate. Responses to photorelease of 8-Br-cAMP by two light flashes of the same intensity, interflash interval 20 s. Currents in the same olfactory sensory neuron were measured at the holding potential of +50 mV (top trace) or −50 mV (bottom trace), corresponding to the calculated reversal potential for chloride. Current amplitudes at +50 mV were similar (80 and 81 pA), whereas at −50 mV, the response to the second flash (−8 pA) was reduced to 36% of the response to the first flash (−22 pA). The small size of the CNG-induced inward current is consistent with previous data showing that in the presence of 1 mM external Ca^{2+}, the ratio between the CNG current at +50 and −50 mV was ∼4 (Fig. 1 of Kleene, 1995) and indicates that in mouse olfactory sensory neurons, high values of inward current are due to Ca^{2+}-activated Cl^- current. Similar results were measured in a total of five olfactory sensory neurons.

second flash was −8 pA, corresponding to 36% of the control response. In these ionic conditions, the response was mainly mediated by a cationic current through CNG channels, and therefore Fig. 9 shows that adaptation was present at the level of CNG channels activated by 8-Br-cAMP. It is of interest to note that the current in control conditions was higher at +50 mV (80 pA) than at −50 mV (−22 pA) (ratio 3.6). The rectification we have measured is consistent with previous reports of the current–voltage relation properties of CNG channels in olfactory cilia. In fact, in the presence of 1 mM Ca^{2+} in the external solution, CNG channels are more strongly inhibited by Ca^{2+} at negative than at positive potentials. From Fig. 1 of Kleene (1995), it can be estimated that in the presence of 1 mM Ca^{2+}, the ratio between the CNG current at +50 and −50 mV was ∼4, very similar to the value we measured in our experimental conditions.

Ca^{2+}-activated Cl^- Channels

To investigate the possibility that response adaptation occurs also on Ca^{2+}-activated Cl^- channels, we produced repetitive intraciliary Ca^{2+} increases to directly activate Cl^- channels by photolysis of caged Ca^{2+} (Fig. 10). In these experiments, the intracellular solution in the patch pipette contained caged Ca^{2+} instead of caged 8-Br-cAMP. We measured the current in response to Ca^{2+} photorelease by flashes of various light intensities and plotted peak current amplitudes as a function of relative light intensity, F. Data were fitted by the Hill equation, Eq. 1. The best fit gave I_{max} = 1250 pA, $F_{1/2}$ = 0.13, and n = 1.5. The average value for n was 1.7 ± 0.3. We estimated the concentration of Ca^{2+} photoreleased in the cilia by comparing data from Fig. 10 with dose–response relations obtained from excised inside-out patches from the knob/cilia in the mouse $K_{1/2}$ = 3.5 μM, n = 1.4 (Reisert et al., 2005) or $K_{1/2}$ = 4.8 μM, n = 1.9 (Pifferi et al., 2006), and we found that the maximal photoreleased concentration of Ca^{2+} varied between 10 and 50 μM.

Fig. 11 shows the response to repetitive photoreleases of Ca^{2+} at interpulse interval of ∼5 s at two light intensities in the same neuron. At both light intensities, the current elicited by the second light flash had approximately the same amplitude as the one measured with the first light flash, showing absence of adaptation. These experiments indicate that repetitive Ca^{2+} increases do not produce a reduced responsiveness of the Ca^{2+}-activated Cl^- channels, but also show that in the small volume of the cilia there was no Cl^- depletion.

DISCUSSION

The aim of this study was to investigate the role of PDE in olfactory fast adaptation. We directly photoreleased 8-Br-cAMP in the cilia of olfactory sensory neurons and

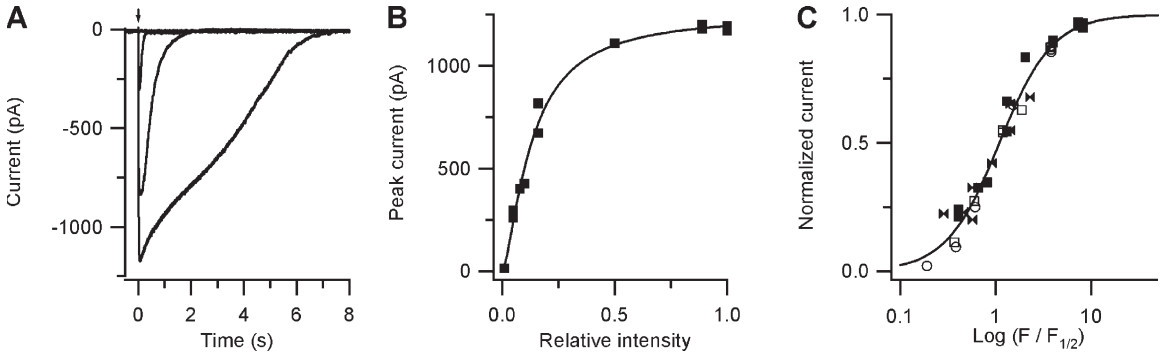

Figure 10. Current responses induced by photorelease of Ca^{2+} as a function of flash intensity. (A) Caged Ca^{2+} (DMNP-EDTA) diffused into the cell from the patch pipette and flashes of increasing intensity were applied to the ciliary region. The arrow indicates the time of application of light flashes of various relative intensities: 0.01, 0.05, 0.16, and 1. Whole-cell current responses were measured at the holding potential of −50 mV. (B) Peak currents from the cell in A were plotted as a function of the relative light intensity, F. The continuous line was the best fit of the Hill Eq. 1 to the data with the following values: I_{max} = 1250 pA, $F_{1/2}$ = 0.13, and n = 1.5. (C) Collected results from four different olfactory sensory neurons. Each symbol represents a different cell. Both axes are normalized values. Normalized peak currents in each cell (I/I_{max}) were plotted versus the logarithm of the relative intensity normalized to the $F_{1/2}$ value ($F/F_{1/2}$) for each cell. The continuous line was the best fit of Eq. 1 to the collected data with n = 1.6. $F_{1/2}$ values ranged between 0.12 and 0.34 and n values varied from 1.4 to 2.1, with an average of 1.7 ± 0.3 (N = 4).

measured adaptation in response to repetitive release of the same ligand concentration (Figs. 4–6). Moreover, we also observed adaptation in double flash experiments in the presence of the PDE inhibitor IBMX (Fig. 8), directly ruling out the hypothesis that PDE activity is significant in fast adaptation. Previous studies have in fact only provided some indirect indication that the hydrolytic activity of PDE is not involved in adaptation. In one study, odorant adaptation has been shown to occur after the synthesis of cAMP and to be consistent with negative feedback modulation by Ca^{2+}-CaM of the CNG channel (Kurahashi and Menini, 1997). Other studies have measured a reduction in current responses induced by repetitive applications of the PDE inhibitor IBMX, giving indirect evidence that PDE is not responsible for adaptation (Ma et al., 1999, 2003; Munger et al., 2001).

Since the increase in intracellular Ca^{2+} concentration also has excitatory effects, because it increases the open probability of Ca^{2+}-activated Cl^- channels, we investigated the contribution to adaptation of the two types of channels responsible for the inward current. We separated CNG currents from Ca^{2+}-activated Cl^- currents by changing the chloride equilibrium potential to the holding potential of −50 mV and found that adaptation was present (Fig. 9). Furthermore, we investigated the possibility that Ca^{2+} has an adapting effect also on Ca^{2+}-activated Cl^- channels by directly activating these channels through photolysis of caged Ca^{2+} (Fig. 10). Currents elicited by repetitive pulses had very similar amplitudes (Fig. 11), indicating that Ca^{2+}-activated Cl^- channels are not directly involved in the adaptation process, consistently with the lack of sensitivity to Ca^{2+}-CaM of Ca^{2+}-activated Cl^- channels measured in intact cilia (Kleene 1999), or in excised patches from knob/cilia of olfactory sensory neurons (Reisert et al., 2003), and with previous experiments on adaptation to odorant stimuli performed in the presence of SITS, a blocker of Ca^{2+}-activated Cl^- current (Kurahashi and Menini, 1997). So, after photorelease of 8-Br-cAMP, its concentration in the cilia should be mainly reduced by diffusion to the

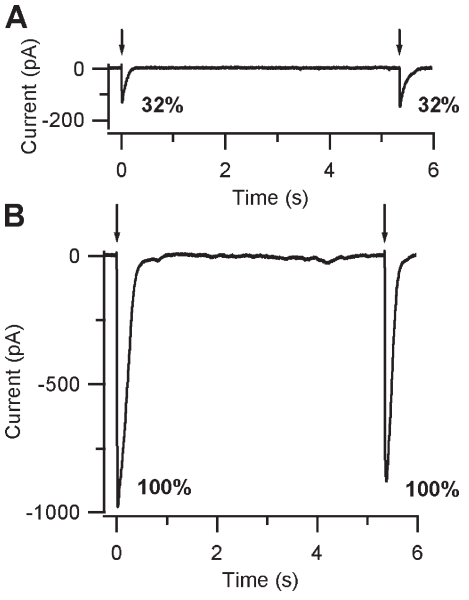

Figure 11. Responses to repetitive photorelease of Ca^{2+}. Whole-cell currents induced by repetitive photorelease of Ca^{2+} (DMNP-EDTA) in an olfactory sensory neuron at −50 mV. The arrows indicate the timing of the light flashes at 0.32 (A) and 1 (B) relative light intensity. Currents elicited by the second flash were very similar to those induced by the first one, indicating the absence of adaptation (130 and 135 pA at 0.32 [A]; 970 and 870 pA at 1 relative light intensity [B]). Three olfactory sensory neurons showed a similar absence of current adaptation to the second photorelease of Ca^{2+}.

dendrite and cell body or by possible binding to buffering sites, rather than by hydrolysis. Indeed, it has been previously estimated that cyclic nucleotides in olfactory cilia can cover a distance of >20 μm in 1 s (Chen et al. 1999; Lagostena and Menini, 2003). Based on these calculations and on the experiments shown in Fig. 3, in which the CNG current in nominally 0 Ca^{2+} returned to baseline within a few seconds, it is likely that 8-Br-cAMP will diffuse away from the cilia in a few seconds after being photoreleased.

Ca^{2+}-CaM Inhibition of the Native Olfactory CNG Channel

Experiments on modulation of the CNG channel by Ca^{2+}-CaM provide an explanation for our results. Bradley et al. (2004, 2005) showed that an endogenous factor, likely apocalmodulin, is already bound to the olfactory CNG channel even in the absence of Ca^{2+} and that when Ca^{2+} concentration becomes higher than 100 nM, Ca^{2+} can rapidly modulate the CNG channel sensitivity by directly binding to the preassociated CaM. Since Ca^{2+} enters into the olfactory cilia through the CNG channel itself, there would be a very fast feedback modulation at the channel level, and therefore Ca^{2+}-CaM inhibition of the CNG channel could be much faster than Ca^{2+}-CaM increase of PDE activity.

But how can the Ca^{2+}-CaM concentration cause a current reduction in the adapted state even several seconds after the first stimulus? When CNG channels were activated by cAMP in excised inside-out patches from knob/cilia of olfactory sensory neurons, the addition of Ca^{2+}-CaM produced a fast current decrease that persisted for several seconds also after CaM was removed in Ca^{2+}-free solution (see Fig. 2 A in Bradley et al. 2001; Fig. 3 [B and E] in Munger et al., 2001; Pifferi et al., 2006). It is likely that this long-lasting inhibition of CNG channels, even after removal of Ca^{2+}-CaM, is the principal molecular mechanism responsible for adaptation to repetitive stimuli. Nevertheless, further studies on the time course and Ca^{2+} dependence of the persistent reduction of sensitivity to cyclic nucleotides of the olfactory CNG channels are required to obtain a better understanding of adaptation.

Quantitative Estimate

To obtain a quantitative estimate of how negative feedback modulation of the CNG channel can describe our experiments we used previously published data obtained in excised inside-out patches from native channels. Balasubramanian et al. (1996) measured the dose–response for both cAMP and 8-Br-cAMP and the modulation by Ca^{2+}-CaM in excised patches from the dendrite knobs of rat olfactory sensory neurons. They discovered that modulation of cyclic nucleotide sensitivity by 0.2 mM Ca^{2+}-CaM was similar whether CNG channels were activated by cAMP or by 8-Br-cAMP. CNG channel sensitivity was greatly reduced by the increase of $K_{1/2}$ of 63-fold (from 3.2 μM to 201 μM) for cAMP and of 84-fold (from 0.3 μM to 31 μM) for 8-Br-cAMP.

In our experimental conditions we have estimated that the maximal concentration of 8-Br-cAMP photoreleased in the cilia was in the range between 5 and 10 μM. By using the Hill parameters obtained by Balasubramanian et al. (1996), the calculated open probability of the CNG channel in the absence of Ca^{2+} is 0.992 at 5 μM and 0.998 at 10 μM 8-Br-cAMP. In the presence of 0.2 mM Ca^{2+}-CaM, the open probability is reduced to 0.23 at 5 μM and to 0.32 at 10 μM 8-Br-cAMP. This calculation shows that even in the presence of high concentrations of 8-Br-cAMP, producing >0.99 channel open probability, it is possible to have a substantial modulation of CNG channel sensitivity and a consequent reduction of current amplitude. The reduction is modulated by the concentrations of Ca^{2+}-CaM. This estimate was based on steady-state measurements of CNG channel dose–response modulated by one concentration of Ca^{2+}-CaM. In physiological conditions Ca^{2+}-CaM modulation is a dynamical process intermingled with activation of Cl^- currents by Ca^{2+}. Recently Reidl et al. (2006) have developed an elegant mathematical model that provides a quantitative dynamical explanation of fast olfactory adaptation based on Ca^{2+}-CaM negative regulation of the CNG channel. Fig. 3 of Reidl et al. (2006) shows that the decrease of free Ca^{2+} concentration was completed within 1 s of the odorant stimulus, whereas the disinhibition of CNG channels by Ca^{2+}-CaM was the slowest process. In the simulation, 4 s after the delivery of the first odorant pulse, 50% of the CNG channels were still inhibited by Ca^{2+}-CaM, producing therefore a reduced response to an identical odorant stimulus, producing the same cyclic nucleotide concentration as in the first pulse. Further experiments and mathematical modeling are required for a more detailed comprehension of how adaptation occurs at molecular level.

Molecular Picture of Ca-dependent Fast Adaptation

Our results are consistent with the following overall molecular picture of how Ca^{2+} causes adaptation. Ca^{2+} enters the cilia through the CNG channels, and the channel sensitivity to cyclic nucleotides is rapidly reduced by Ca^{2+}-CaM modulation. As a consequence, CNG channel open probability could be significantly reduced for several seconds. The increase in intraciliary free Ca^{2+} concentration will also cause an additional inward current due to Ca^{2+}-activated Cl^- channels. After a first increase, the intraciliary free Ca^{2+} concentration will decrease both because Ca^{2+} is continuously extruded via the Na^+/Ca^{2+} exchanger, and because its entry will be progressively reduced by the inhibition of CNG channels caused by Ca^{2+}-CaM. As the intraciliary Ca^{2+} concentration decreases, Ca^{2+}-activated

Cl^- channels will progressively close. CNG channel inhibition by Ca^{2+}-CaM persists for several seconds even in free 0 Ca^{2+} solutions (Bradley et al., 2001; Munger et al., 2001). Thus, in the adapted state, CNG channels are partially inhibited and therefore the same cyclic nucleotide concentration as in the control state produces a lower CNG channel open probability and, as a consequence, a smaller current. The decrease in CNG channel open probability due to Ca^{2+}-CaM can be overcome with a higher cyclic nucleotide concentration, explaining in this way how an olfactory neuron can have a broader dynamic range.

In physiological conditions, cAMP concentration in the cilia is likely to be decreased both by the increased hydrolytic PDE1C2 activity due to Ca^{2+}-CaM and by diffusion to the dendrite and cell body.

In conclusion, our experiments contribute to the present understanding of the molecular mechanisms underlying fast adaptation of olfactory sensory neurons to repetitive stimuli, by providing direct evidence that PDE is not responsible for this process. Whether or not PDE activity is involved in adaptation to long odorant exposures is still an open question.

We thank Simone Pifferi, Giulietta Pinato, Hiroko Takeuchi, and Takashi Kurahashi for helpful discussions, Lara Masten for the preparation of dissociated mouse olfactory sensory neurons, Simone Pifferi for sharing results before publication, and Manuela Schipizza-Lough for checking the English.

This work was supported by the NFG grant n. 503221 (to A.M.) from the European Community.

Olaf S. Andersen served as editor.

Submitted: 7 April 2006
Accepted: 23 June 2006

REFERENCES

Balasubramanian, S., J.W. Lynch, and P.H. Barry. 1996. Calcium-dependent modulation of the agonist affinity of the mammalian olfactory cyclic nucleotide-gated channel by calmodulin and a novel endogenous factor. *J. Membr. Biol.* 152:13–23.

Beltman, J., D.E. Becker, E. Butt, G.S. Jensen, S.D. Rybalkin, B. Jastorff, and J.A. Beavo. 1995. Characterization of cyclic nucleotide phosphodiesterases with cyclic GMP analogs: topology of the catalytic domains. *Mol. Pharmacol.* 47:330–339.

Boekhoff, I., C. Kroner, and H. Breer. 1996. Calcium controls second-messenger signalling in olfactory cilia. *Cell. Signal.* 8:167–171.

Borisy, F.F., G.V. Ronnett, A.M. Cunningham, D. Juilfs, J. Beavo, and S.H. Snyder. 1992. Calcium/calmodulin-activated phosphodiesterase expressed in olfactory receptor neurons. *J. Neurosci.* 12:915–923.

Bradley, J., W. Bonigk, K.W. Yau, and S. Frings. 2004. Calmodulin permanently associates with rat olfactory CNG channels under native conditions. *Nat. Neurosci.* 7:705–710.

Bradley, J., J. Reisert, and S. Frings. 2005. Regulation of cyclic nucleotide-gated channels. *Curr. Opin. Neurobiol.* 15:343–349.

Bradley, J., D. Reuter, and S. Frings. 2001. Facilitation of calmodulin-mediated odor adaptation by cAMP-gated channel subunits. *Science.* 294:2176–2178.

Braumann, T., C. Erneux, G. Petridis, W.D. Stohrer, and B. Jastorff. 1986. Hydrolysis of cyclic nucleotides by a purified cGMP-stimulated phosphodiesterase: structural requirements for hydrolysis. *Biochim. Biophys. Acta.* 871:199–206.

Butt, E., J. Beltman, D.E. Becker, G.S. Jensen, S.D. Rybalkin, B. Jastorff, and J.A. Beavo. 1995. Characterization of cyclic nucleotide phosphodiesterases with cyclic AMP analogs: topology of the catalytic sites and comparison with other cyclic AMP-binding proteins. *Mol. Pharmacol.* 47:340–347.

Chen, C., T. Nakamura, and Y. Koutalos. 1999. Cyclic AMP diffusion coefficient in frog olfactory cilia. *Biophys. J.* 76:2861–2867.

Chen, S., A.P. Lane, R. Bock, T. Leinders-Zufall, and F. Zufall. 2000. Blocking adenylyl cyclase inhibits olfactory generator currents induced by "IP(3)-odors". *J. Neurophysiol.* 84:575–580.

Chen, T.Y., and K.W. Yau. 1994. Direct modulation by Ca^{2+}-calmodulin of cyclic nucleotide-activated channel of rat olfactory receptor neurons. *Nature.* 368:545–548.

Dubin, A.E., and V.E. Dionne. 1994. Action potentials and chemosensitive conductances in the dendrites of olfactory neurons suggest new features for odor transduction. *J. Gen. Physiol.* 103:181–201.

Firestein, S. 2001. How the olfactory system makes sense of scents. *Nature.* 413:211–218.

Firestein, S., B. Darrow, and G.M. Shepherd. 1991a. Activation of the sensory current in salamander olfactory receptor neurons depends on a G protein-mediated cAMP second messenger system. *Neuron.* 6:825–835.

Firestein, S., F. Zufall, and G.M. Shepherd. 1991b. Single odor-sensitive channels in olfactory receptor neurons are also gated by cyclic nucleotides. *J. Neurosci.* 11:3565–3572.

Frings, S., D. Reuter, and S.J. Kleene. 2000. Neuronal Ca^{2+}-activated Cl^- channels-homing in on an elusive channel species. *Prog. Neurobiol.* 60:247–289.

Guellaen, G., J.L. Mahu, P. Mavier, P. Berthelot, and J. Hanoune. 1977. RMI 12330 A, an inhibitor of adenylate cyclase in rat liver. *Biochim. Biophys. Acta.* 484:465–475.

Hagen, V., J. Bendig, S. Frings, T. Eckardt, S. Helm, D. Reuter, and U.B. Kaupp. 2001. Highly efficient and ultrafast phototriggers for cAMP and cGMP by using long-wavelength UV/Vis-activation. *Angew. Chem. Int. Ed. Engl.* 40:1045–1048.

Hagen, V., K. Benndorf, and U.B. Kaupp. 2005. Photochemical release of second messengers-caged cyclic nucleotides. *In* Dynamic Studies in Biology: Phototriggers, Photoswitches and Caged Biomolecules. M. Goeldner and R.S. Givens, editors. Wiley-VCH, Weinheim, Germany. 155–178.

Harris, D.N., M.M. Asaad, M.B. Phillips, H.J. Goldenberg, and M.J. Antonaccio. 1979. Inhibition of adenylate cyclase in human blood platelets by 9-substituted adenine derivatives. *J. Cyclic Nucleotide Res.* 5:125–134.

Jung, A., F.W. Lischka, J. Engel, and D. Schild. 1994. Sodium/calcium exchanger in olfactory receptor neurones of *Xenopus laevis*. *Neuroreport.* 5:1741–1744.

Kaneko, H., I. Putzier, S. Frings, U.B. Kaupp, and T. Gensch. 2004. Chloride accumulation in mammalian olfactory sensory neurons. *J. Neurosci.* 24:7931–7938.

Kaupp, U.B., and R. Seifert. 2002. Cyclic nucleotide-gated ion channels. *Physiol. Rev.* 82:769–824.

Kleene, S.J. 1993. Origin of the chloride current in olfactory transduction. *Neuron.* 11:123–132.

Kleene, S.J. 1995. Block by external calcium and magnesium of the cyclic-nucleotide-activated current in olfactory cilia. *Neuroscience.* 66:1001–1008.

Kleene, S.J. 1999. Both external and internal calcium reduce the sensitivity of the olfactory cyclic-nucleotide-gated channel to cAMP. *J. Neurophysiol.* 81:2675–2682.

Kleene, S.J., and R.C. Gesteland. 1991. Calcium-activated chloride conductance in frog olfactory cilia. *J. Neurosci.* 11:3624–3629.

Kramer, R.H., and S.A. Siegelbaum. 1992. Intracellular Ca^{2+} regulates the sensitivity of cyclic nucleotide-gated channels in olfactory receptor neurons. *Neuron.* 9:897–906.

Kurahashi, T., and A. Menini. 1997. Mechanism of odorant adaptation in the olfactory receptor cell. *Nature.* 385:725–729.

Kurahashi, T., and T. Shibuya. 1990. Ca^{2+}-dependent adaptive properties in the solitary olfactory receptor cell of the newt. *Brain Res.* 515:261–268.

Kurahashi, T., and K.W. Yau. 1993. Co-existence of cationic and chloride components in odorant-induced current of vertebrate olfactory receptor cells. *Nature.* 363:71–74.

Lagostena, L., and A. Menini. 2003. Whole-cell recordings and photolysis of caged compounds in olfactory sensory neurons isolated from the mouse. *Chem. Senses.* 28:705–716.

Leinders-Zufall, T., C.A. Greer, G.M. Shepherd, and F. Zufall. 1998. Imaging odor-induced calcium transients in single olfactory cilia: specificity of activation and role in transduction. *J. Neurosci.* 18:5630–5639.

Lowe, G., and G.H. Gold. 1993a. Nonlinear amplification by calcium-dependent chloride channels in olfactory receptor cells. *Nature.* 366:283–286.

Lowe, G., and G.H. Gold. 1993b. Contribution of the ciliary cyclic nucleotide-gated conductance to olfactory transduction in the salamander. *J. Physiol.* 462:175–196.

Ma, M., W.R. Chen, and G.M. Shepherd. 1999. Electrophysiological characterization of rat and mouse olfactory receptor neurons from an intact epithelial preparation. *J. Neurosci. Methods.* 92:31–40.

Ma, M., X. Grosmaitre, C.L. Iwema, H. Baker, C.A. Greer, and G.M. Shepherd. 2003. Olfactory signal transduction in the mouse septal organ. *J. Neurosci.* 23:317–324.

Matthews, H.R., and J. Reisert. 2003. Calcium, the two-faced messenger of olfactory transduction and adaptation. *Curr. Opin. Neurobiol.* 13:469–475.

Menini, A. 1999. Calcium signalling and regulation in olfactory neurons. *Curr. Opin. Neurobiol.* 9:419–426.

Menini, A., L. Lagostena, and A. Boccaccio. 2004. Olfaction: from odorant molecules to the olfactory cortex. *News Physiol. Sci.* 19:101–104.

Munger, S.D., A.P. Lane, H. Zhong, T. Leinders-Zufall, K.W. Yau, F. Zufall, and R.R. Reed. 2001. Central role of the CNGA4 channel subunit in Ca^{2+}-calmodulin-dependent odor adaptation. *Science.* 294:2172–2175.

Nickell, W.T., N.K. Kleene, R.C. Gesteland, and S.J. Kleene. 2006. Neuronal chloride accumulation in olfactory epithelium of mice lacking NKCC1. *J. Neurophysiol.* 95:2003–2006.

Pifferi, S., A. Boccaccio, and A. Menini. 2006. Cyclic nucleotide-gated ion channels in sensory transduction. *FEBS Lett.* DOI:10.1016/j.febslet.2006.03.086.

Reidl, J., P. Borowski, A. Sensse, J. Starke, M. Zapotocky, and M. Eiswirth. 2006. Model of calcium oscillations due to negative feedback in olfactory cilia. *Biophys. J.* 90:1147–1155.

Reisert, J., J. Lai, K.W. Yau, and J. Bradley. 2005. Mechanism of the excitatory Cl^- response in mouse olfactory receptor neurons. *Neuron.* 45:553–561.

Reisert, J., and H.R. Matthews. 1998. Na^+-dependent Ca^{2+} extrusion governs response recovery in frog olfactory receptor cells. *J. Gen. Physiol.* 112:529–535.

Reisert, J., and H.R. Matthews. 1999. Adaptation of the odour-induced response in frog olfactory receptor cells. *J. Physiol.* 519:801–813.

Reisert, J., and H.R. Matthews. 2001. Response properties of isolated mouse olfactory receptor cells. *J. Physiol.* 530:113–122.

Reisert, J., P.J. Bauer, K.W. Yau, and S. Frings. 2003. The Ca-activated Cl channel and its control in rat olfactory receptor neurons. *J. Gen. Physiol.* 122:349–363.

Reuter, D., K. Zierold, W.H. Schroder, and S. Frings. 1998. A depolarizing chloride current contributes to chemoelectrical transduction in olfactory sensory neurons in situ. *J. Neurosci.* 18:6623–6630.

Schild, D., and D. Restrepo. 1998. Transduction mechanisms in vertebrate olfactory receptor cells. *Physiol. Rev.* 78:429–466.

Takeuchi, H., and T. Kurahashi. 2002. Photolysis of caged cyclic AMP in the ciliary cytoplasm of the newt olfactory receptor cell. *J. Physiol.* 541:825–833.

Takeuchi, H., and T. Kurahashi. 2003. Identification of second messenger mediating signal transduction in the olfactory receptor cell. *J. Gen. Physiol.* 122:557–567.

Takeuchi, H., and T. Kurahashi. 2005. Mechanism of signal amplification in the olfactory sensory cilia. *J. Neurosci.* 25:11084–11091.

Torre, V., J.F. Ashmore, T.D. Lamb, and A. Menini. 1995. Transduction and adaptation in sensory receptor cells. *J. Neurosci.* 15:7757–7768.

Trudeau, M.C., and W.N. Zagotta. 2003. Calcium/calmodulin modulation of olfactory and rod cyclic nucleotide-gated ion channels. *J. Biol. Chem.* 278:18705–18708.

Wayman, G.A., S. Impey, and D.R. Storm. 1995. Ca^{2+} inhibition of type III adenylate cyclase in vivo. *J. Biol. Chem.* 270:21480–21486.

Wei, J., G. Wayman, and D.R. Storm. 1996. Phosphorylation and inhibition of type III adenylate cyclase by calmodulin-dependent protein kinase II in vivo. *J. Biol. Chem.* 271:24231–24235.

Wei, J., A.Z. Zhao, G.C. Chan, L.P. Baker, S. Impey, J.A. Beavo, and D.R. Storm. 1998. Phosphorylation and inhibition of olfactory adenylate cyclase by CaM kinase II in neurons: a mechanism for attenuation of olfactory signals. *Neuron.* 21:495–504.

Yan, C., A.Z. Zhao, J.K. Bentley, K. Loughney, K. Ferguson, and J.A. Beavo. 1995. Molecular cloning and characterization of a calmodulin-dependent phosphodiesterase enriched in olfactory sensory neurons. *Proc. Natl. Acad. Sci. USA.* 92:9677–9681.

Zimmerman, A.L., G. Yamanaka, F. Eckstein, D.A. Baylor, and L. Stryer. 1985. Interaction of hydrolysis-resistant analogs of cyclic GMP with the phosphodiesterase and light-sensitive channel of retinal rod outer segments. *Proc. Natl. Acad. Sci. USA.* 82:8813–8817.